Monthly Notices of the ROYAL ASTRONOMICAL SOCIETY

MNRAS **449,** 4277–4287 (2015) doi:10.1093/mnras/stv589

# Galaxy And Mass Assembly (GAMA) blended spectra catalogue: strong galaxy–galaxy lens and occulting galaxy pair candidates

B. W. Holwerda,[1⋆] I. K. Baldry,[2] M. Alpaslan,[3] A. Bauer,[4] J. Bland-Hawthorn,[5] S. Brough,[4] M. J. I. Brown,[6] M. E. Cluver,[7] C. Conselice,[8] S. P. Driver,[9,10] A. M. Hopkins,[4] D. H. Jones,[11] Á. R. López-Sánchez,[4,11] J. Loveday,[12] M. J. Meyer[9] and A. Moffett[9]

[1] *University of Leiden, Sterrenwacht Leiden, Niels Bohrweg 2, NL-2333 CA Leiden, the Netherlands*
[2] *Astrophysics Research Institute, Liverpool John Moores University, IC2, Liverpool Science Park, 146 Brownlow Hill, Liverpool L3 5RF, UK*
[3] *NASA Ames Research Centre, N232, Moffett Field, Mountain View, CA 94034, USA*
[4] *Australian Astronomical Observatory, 105 Delhi Rd, North Ryde, NSW 2113, Australia*
[5] *Sydney Institute for Astronomy, School of Physics A28, University of Sydney, NSW 2006, Australia*
[6] *School of Physics, Monash University, Clayton, Vic 3800, Australia*
[7] *Department of Physics, University of the Western Cape, Robert Sobukwe Road, Bellville 7530, South Africa*
[8] *University of Nottingham, School of Physics & Astronomy, Nottingham NG7 2RD, UK*
[9] *ICRAR M468, University of Western Australia, 35 Stirling Hwy, Crawley, WA 6009, Australia*
[10] *School of Physics & Astronomy, University of St Andrews, North Haugh, St Andrews KY16 9SS, Scotland*
[11] *Department of Physics and Astronomy, Macquarie University, NSW 2109, Australia*
[12] *Astronomy Centre, University of Sussex, Falmer, Brighton BN1 9QH, UK*

Accepted 2015 March 16. Received 2015 March 16; in original form 2014 December 17

## ABSTRACT

We present the catalogue of blended galaxy spectra from the Galaxy And Mass Assembly (GAMA) survey. These are cases where light from two galaxies are significantly detected in a single GAMA fibre. Galaxy pairs identified from their blended spectrum fall into two principal classes: they are either strong lenses, a passive galaxy lensing an emission-line galaxy; or occulting galaxies, serendipitous overlaps of two galaxies, of any type. Blended spectra can thus be used to reliably identify strong lenses for follow-up observations (high-resolution imaging) and occulting pairs, especially those that are a late-type partly obscuring an early-type galaxy which are of interest for the study of dust content of spiral and irregular galaxies. The GAMA survey setup and its AUTOZ automated redshift determination were used to identify candidate blended galaxy spectra from the cross-correlation peaks. We identify 280 blended spectra with a minimum velocity separation of 600 km s$^{-1}$, of which 104 are lens pair candidates, 71 emission-line-passive pairs, 78 are pairs of emission-line galaxies and 27 are pairs of galaxies with passive spectra. We have visually inspected the candidates in the Sloan Digital Sky Survey (SDSS) and Kilo Degree Survey (KiDS) images. Many blended objects are ellipticals with blue fuzz (*Ef* in our classification). These latter 'Ef' classifications are candidates for possible strong lenses, massive ellipticals with an emission-line galaxy in one or more lensed images. The GAMA lens and occulting galaxy candidate samples are similar in size to those identified in the entire SDSS. This blended spectrum sample stands as a testament of the power of this highly complete, second-largest spectroscopic survey in existence and offers the possibility to expand e.g. strong gravitational lens surveys.

**Key words:** gravitational lensing: strong – catalogues – dust, extinction – galaxies: distances and redshifts – galaxies: statistics.

## 1 INTRODUCTION

Interstellar dust is still a dominant astrophysical unknown in cosmological distance estimates (Albrecht et al. 2006; Holwerda 2008; Holwerda et al. 2014) and models of how starlight is re-processed

⋆ E-mail: benne.holwerda@gmail.com

within a galaxy (e.g. Baes et al. 2010; Bianchi & Xilouris 2011; Popescu et al. 2011; de Looze et al. 2012; Holwerda et al. 2012) because some 10–30 per cent of all the starlight is re-emitted by the dust in the far-infrared (Popescu et al. 2000). Interstellar dust can be found in two ways; by its emission or through the extinction of stellar light.

Characterization of emission has made great strides with the *Spitzer* and *Herschel Space Observatories* (e.g. Hinz et al. 2009, 2012; Bendo et al. 2012, 2015; Baes et al. 2010; Smith et al. 2010; Galametz et al. 2012; Xilouris et al. 2012; Verstappen et al. 2013; Draine et al. 2014; Hughes et al. 2014, 2015). A library of far-infrared and sub-mm images of nearby galaxies is currently being collated and more insight into the physics and distribution of interstellar dust in nearby galaxies can be expected with the great improvements in spectral coverage, sensitivity and spatial resolution.

Extinction measures of dust have some specific advantages over emission; they do not depend on the dust temperature, allowing for the detection of much colder dusty structures, and typically have the high resolution of the optical imaging observations. The single drawback is that one needs a known background light source. In the case of the transparency of spiral galaxies, two techniques have just such a proven background source: background galaxies counts and occulting galaxy pairs. The technique that uses the number of background galaxies (González et al. 1998, 2003; Cuillandre et al. 2001; Holwerda 2005; Holwerda et al. 2005a,b,c,e,d, 2007b,a, 2013) is nearing obsolescence as its inherent resolution and accuracy, limited by the intrinsic cosmic variance of background sources, are now surpassed by the accuracy and sensitivity of *Herschel Space Observatory* observations of dust surface density in nearby galaxies.

The occulting galaxies technique, however, has increased steadily in accuracy and usefulness, owing in a large part to the increasing sample sizes. Estimating dust extinction and mass from differential photometry in occulting pairs of galaxies was first proposed by White & Keel (1992). Their technique was then applied to all known pairs using ground-based optical images (Andredakis & van der Kruit 1992; Berlind et al. 1997; Domingue et al. 1999; White, Keel & Conselice 2000) and spectroscopy (Domingue, Keel & White 2000). Subsequently, some pairs were imaged with the *Hubble Space Telescope* (*HST*; Elmegreen et al. 2001; Keel & White 2001a,b; Holwerda et al. 2009; Holwerda & Keel 2013). These initial results, however, were limited by sample sizes (∼15 pairs). More recently, new pairs were found in the Sloan Digital Sky Survey (SDSS) spectroscopic catalogue (86 pairs in Holwerda, Keel & Bolton 2007c) and through the GalaxyZOO project (Lintott et al. 2008); 1993 pairs reported in Keel et al. (2013). This wealth of new pairs provided opportunities for follow-up with IFU observations (Holwerda & Keel 2013; Holwerda et al. 2013) and *GALEX* (Keel et al. 2014). A greatly expanded occulting galaxy catalogue improves accuracy as 'ideal pairs' – an elliptical partially occulted by a late-type galaxy – can be selected for follow-up. Ellipticals are the optimal background source as their light profile is smooth and very symmetric.[1]

Results from the occulting galaxy pairs include: (1) a mean extinction profile (Domingue et al. 2000; White et al. 2000; Holwerda et al. 2007c), (2) an indication that the dust may be fractal (Keel & White 2001a) and (3) the observation that the colour-extinction relation is grey, i.e. there is little or no relation between the reddening of the stellar populations and total extinction. The latter is due to the coarse physical sampling of ground-based observations. The Galactic extinction law returns as soon as the physical sampling of the overlap region resolves the molecular clouds in the foreground disc (<100 pc Elmegreen et al. 2001; Keel & White 2001a,b; Holwerda et al. 2009).

A very reliable way to identify occulting galaxy pairs, i.e. purely serendipitous overlaps of galaxies is through blended spectra. In Holwerda et al. (2007c), we used the rejects from the Strong Lenses with ACS Survey (SLACS; Bolton et al. 2004, 2006), a highly successful search for strong lenses, confirmed with *HST* (Koopmans et al. 2006; Treu et al. 2006, 2009; Gavazzi et al. 2007, 2008; Bolton et al. 2008a,b), with spectroscopic selection extended now to the BOSS survey (Bolton et al. 2012; Brownstein et al. 2012). Both types of blended spectral sources have two things in common, very close association on the sky (within an SDSS spectroscopic fibre of 3 arcsec diameter) and clear spectroscopic signal from both galaxies at distinct redshifts.

In this paper, we present the blended spectra catalogue based on the Galaxy And Mass Assembly (GAMA) survey (Driver et al. 2009, 2011; Baldry et al. 2010) as candidates for either strong lensing follow-up or occulting galaxy analysis (e.g. *HST* imaging or spectroscopy). The GAMA data is an improvement over SDSS as the target galaxies can be fainter, the aperture is smaller (i.e. a closer overlap of the galaxies) and the AUTOZ detection algorithm is a marked improvement on the SDSS detections. The paper is organized as follows. Section 2 briefly introduces the GAMA survey, Section 3 the redshift determination and selection of blended spectra, Section 4 presents the visual classifications of the blended objects, Section 5 presents the blended spectra catalogue and we discuss the pair classification and their possible future uses in Section 6.

## 2 GAMA SURVEY

The GAMA survey has obtained over 250 000 galaxy redshifts selected to $r < 19.8$ mag over 290 deg$^2$ of sky (Driver et al. 2009, 2011; Baldry et al. 2010; Liske 2015). At the heart of this survey is the redshift survey with the upgraded 2dF spectrograph AAOmega (Saunders et al. 2006; Sharp et al. 2006) on the Anglo-Australian Telescope. The GAMA survey extends over three equatorial survey regions of 60 deg$^2$ each (called G09, G12 and G15) and two Southern regions of similar area (G02, G23). See Baldry et al. (2010) for a detailed description of the GAMA input catalogue for the equatorial regions.

The redshift survey in combination with a wealth of imaging data has led to many science results already. We use for this work the GAMA II redshifts (Liske 2015), which were obtained using a robust cross-correlation method for spectra with and without strong emission lines (Baldry et al. 2014).

## 3 SELECTION OF BLENDED SPECTRA

Galaxy redshifts were initially determined by a supervised fit (Liske 2015) but a recent upgrade to the GAMA survey pipeline includes a fully automated template-based redshift determination (AUTOZ; Baldry et al. 2014). In certain cases, the fits for different templates resulted in two high fidelity, but different redshifts; these are the candidate blended objects of interest to us here.

The AUTOZ code obtains cross-correlation redshifts against stellar and galaxy templates with varying strength of emission and absorption line features. The height and position of the first four peaks

[1] The one exception is where we attempt to measure blue light attenuation. In this case, a spiral galaxy, which is brighter in the blue, is preferred.

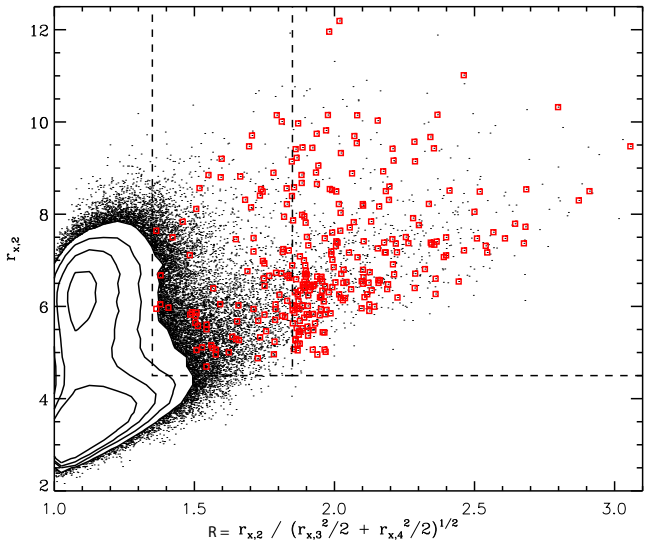


**Figure 1.** Distribution in selection parameters: for all GAMA spectra shown with contours and black points, and selected candidates shown with red squares. Note the all GAMA sample includes star–galaxy blends. The main selection criteria was $\mathcal{R} > 1.85$ and this results in $r_{x,2} > 4.5$ by default. Candidates from an earlier version of the code have $\mathcal{R}$ between 1.35 and 1.85. These boundaries are shown with dashed lines.

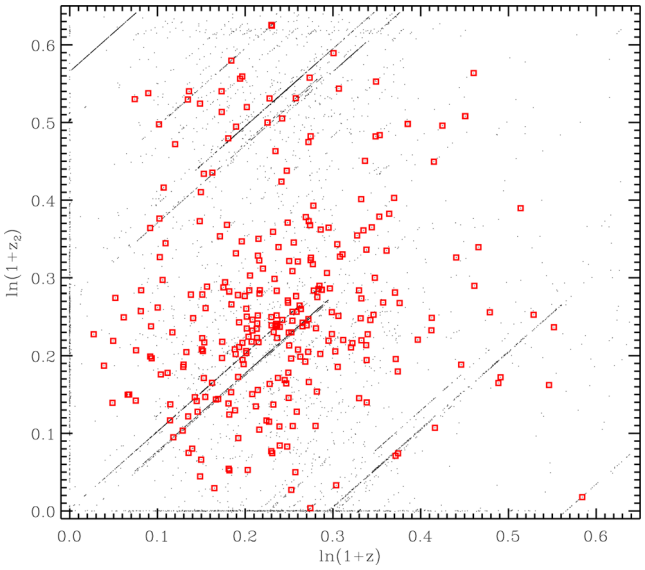


**Figure 2.** Distribution in $z_2$ versus $z$: for all GAMA spectra with $\mathcal{R} > 1.35$ and $r_{x,2} > 4.5$ shown with black points, and for the selected candidates($\mathcal{R} > 1.85$) shown with red squares. Most candidates lie away from the alias lines that are appearing parallel when plotting the logarithm of one plus redshift on each axis.

of normalized cross-correlation functions are obtained. These are called $r_x$, $r_{x,2}$, $r_{x,3}$ and $r_{x,4}$ each with a corresponding redshift and template number, with the peaks separated by at least 600 km s$^{-1}$. High values of $r_x$ and $r_{x,2}$, particularly relative to $r_{x,3}$ and $r_{x,4}$, can then be used to select candidate blended spectra.

The AUTOZ algorithm marks a significant improvement in the identification of blended spectra over that which could be obtained from GAMA I redshifts. In the initial redshift campaign, 'redshifters' – the GAMA team members identifying the redshift with RUNZ – were focused on attaining a reliable redshift for single objects. In such an approach, only those spectra with wildly different redshifts by two redshifters or spectra remarked upon during visual inspection would be selected. With AUTOZ, blended spectra are identified as different redshifts using normalized cross-correlation functions, a much more objective and complete approach.

### 3.1 AUTOZ selection

Double redshift selection using the AUTOZ approach was to require that two different redshifts had high cross-correlation peaks ($r_x$ and $r_{x,2}$), while the next two redshifts had significantly lower peak values. In order to address this, we defined the ratio between the second redshift peak value and subsequent, third and fourth, redshift peaks to be

$$\mathcal{R} = r_{x,2} \Big/ \sqrt{(r_{x,3}^2 + r_{x,4}^2)}. \quad (1)$$

To select the double-$z$ candidates, we required $\mathcal{R} > 1.85$ (to avoid aliasing and a clean selection of real blends, see Figs 1 and 2) and for the first two redshifts to be from galaxy spectral templates. The galaxy spectral templates used in AUTOZ were from SDSS. An early version of the code used the SDSS DR2 templates, while a later version used templates derived from the Bolton et al. (2012) galaxy eigenspectra. These later templates were numbered 40–47 in order of increasing emission-line strength. To broadly classify the templates, we select templates 40–42 as 'passive galaxies' (PG) and 43–47 as 'emission-line galaxies' (ELG).

**Table 1.** The numbers of different blended spectra identified in GAMA using the AUTOZ algorithm.

| Pair Type | Number |
|---|---|
| ELG+ELG | 78 |
| ELG+PG | 71 |
| PG+ELG | 104 |
| PG+PG | 27 |
| Total | 280 |

Initially, we selected candidates with $\mathcal{R} > 1.85$ and $r_{x,2} > 5.5$, with these values determined using the early version of the code. After the code was updated, the value of $\mathcal{R}$ changed as a result of the new templates and a modest increase in the allowed redshift range from 0.8 to 0.9. Using the new values, we selected candidates with $\mathcal{R} > 1.85$ and with no restriction on $r_{x,2}$. Old candidates were retained subject to a couple of criteria; the new value of $\mathcal{R}$ was still greater than 1.35, and $(1 + z)/(1 + z_2)$ was not near a problematic cross-correlation alias. Aliases can result from the matching of different emission lines in the templates to a strong line in the data. All candidates, old and new, near the alias of $(1 + z)/(1 + z_2) = 1.343 \pm 0.002$ (∼5007/3727) or the inverse were removed from the sample. Fig. 1 shows the distribution of candidates in $r_{x,2}$ versus $\mathcal{R}$, i.e. the selection parameters. Fig. 2 shows where the aliases lie, in $z_2$ versus $z$, with respect to the candidates.

The selection resulted in 280 galaxy pair candidates (from 299 blended spectra – some source locations were observed more than once). Depending on which template matched best for both redshifts in the blend, we classified the type of blends as follows: two passive-template galaxies (PG+PG), two emission-line templates (ELG+ELG), a passive template at low redshift and emission line template at higher redshift (PG+ELG), or vice versa (ELG+PG). Table 1 summarizes the resulting classifications. The AUTOZ results for our 280 blended objects are listed in Table 3.

**Table 2.** The Keel et al. (2013) classification of the occulting galaxy pairs.

| Classification | Description |
|---|---|
| F | Spirals seen nearly face-on in front of an elliptical or S0 background system. |
| Q | The background galaxy is nearly edge-on and is projected nearly radial. |
| Φ | The spiral is seen essentially edge-on, at least partially backlit by a smooth galaxy. |
| X | Two edge-on disc galaxies |
| SE | Spiral in front of an Elliptical, not in one of the above categories. |
| S | Spiral/spiral overlaps. |
| B | The background galaxy has much smaller angular size than the foreground disc. |
| E | Pairs containing only elliptical or S0 galaxies. |

## 4 VISUAL CLASSIFICATION

We visually classified all the 280 galaxy pairs identified by AUTOZ using the SDSS image viewer and GAMA cutouts in the case of the Southern fields. We classify whether the object appears as a single galaxy (either S or E, where S can mean a spiral galaxy or an irregular one i.e. late type, except in a few clear cases and E an early type), an occulting pair or a disturbed ongoing merger (M). We subclassify the occulting pair similar to the Keel et al. (2013) classification (Table 2) but given the limited image resolution the classification is essentially S-E, S-S or E-E. We introduce a subclassification for single early types with some blue fuzzy hue on one side of the SDSS *gri* composite galaxy images (Ef). These latter could be lensing ellipticals or simply occulting pairs with a very small irregular galaxy in the foreground or background.

The classifications are listed in Table 2. Fig. 3 shows the distribution of visual classifications of the blended spectrum objects. One would expect a reasonable correlation between the spectral typing (e.g. passive versus emission-line) with the visual classifications, e.g. passive spectra dominating those pairs with an E type galaxy in the foreground. The relation between visual classification and spectral classification is tenuous. Visual classification based on colour images can be both powerful but also misleading. Blue galaxies tend to be classified as late types even if their profile is actually that of a spheroid.

With this in mind, two of us (BWH and AM) reclassified *sdss-i* postage stamps from the KiLO Degree Survey (KiDS) survey (de Jong et al. 2013). Fig. 4 shows the distribution of these visual classifications. Because these are single-filter, the classification *Bf* is

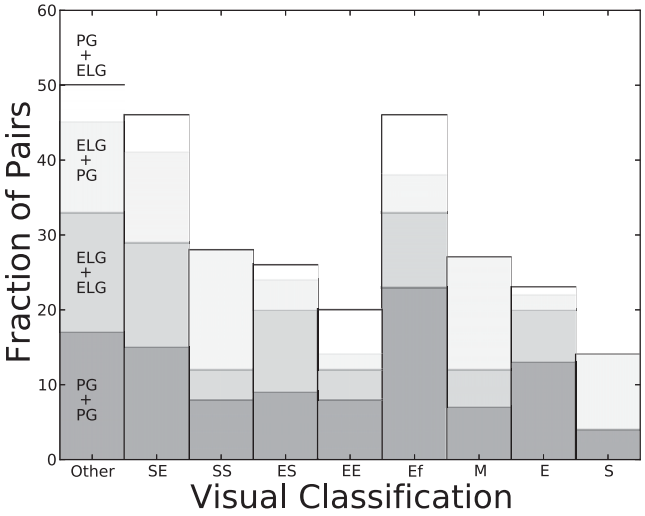


**Figure 3.** The distribution of visual classifications for all the blended spectra broken down into all four possible template combinations (PG=passive template, ELG=emission line template, PG+ELG is a passive in front of an emission line pair). No clear correlation between the SDSS visual classifications and the template ones is evident. The 'other' category are objects without SDSS imaging or a reasonable classification.

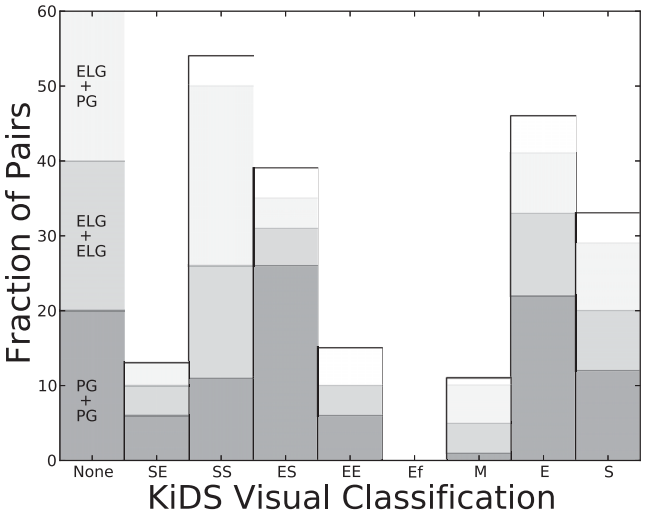


**Figure 4.** The distribution of visual classifications of the KiDS *sdss-i* filter for all the blended spectra broken down into all four possible template combinations (PG=passive template, ELG=emission line template, PG+ELG is a passive in front of an emission line pair). The lack of a correlation between visual and spectral classification persist with the singe-filter classifications.

**Table 3.** The complete catalogue of blended spectra in the GAMA survey. T1 and T2 refer to the template numbers for the first and second peaks. The full catalogue is available in the online publication only.

| Field | GAMA-id | RA | Dec. | $z$ | T1 | $r_x$ | $z_2$ | T2 | $r_{x,2}$ | Spec. Type | Vis. type |
|---|---|---|---|---|---|---|---|---|---|---|---|
| G09 | 196060 | 129.016 21 | −0.693 36 | 0.293 | 40 | 8.7 | 0.051 | 46 | 5.6 | ELG+PG | SE |
| G09 | 197073 | 133.781 79 | −0.747 90 | 0.270 | 40 | 10.8 | 0.268 | 44 | 6.4 | ELG+PG | EE |
| G09 | 198082 | 138.281 50 | −0.666 73 | 0.163 | 40 | 11.1 | 0.321 | 47 | 10.2 | PG+ELG | ES |
| G09 | 202448 | 129.695 46 | −0.381 79 | 0.418 | 40 | 9.0 | 0.738 | 45 | 5.0 | PG+ELG | SE |
| G09 | 204140 | 136.638 83 | −0.352 03 | 0.282 | 40 | 9.4 | 0.449 | 47 | 8.1 | PG+ELG | Ef |
| G09 | 209222 | 132.367 71 | 0.163 60 | 0.128 | 40 | 10.3 | 0.603 | 47 | 6.7 | PG+ELG | E |
| G09 | 209263 | 132.505 96 | 0.042 50 | 0.310 | 42 | 6.5 | 0.270 | 46 | 5.3 | ELG+PG | Ef |
| G09 | 209295 | 132.610 13 | 0.119 72 | 0.313 | 40 | 11.2 | 0.608 | 47 | 7.8 | PG+ELG | Ef |
| ... | ... | ... | ... | ... | ... | ... | ... | ... | ... | ... | ... |

impossible. The new visual classifications remains poorly correlated with the spectral classification.

In our opinion, both the SDSS colour-images or the deeper and higher resolution KiDS single-filter images are still too low resolution to unambiguously disentangle and visually classify these objects. These objects are inherently blended ones. Even with another improvement in spatial resolution (i.e. *HST* imaging), visual classifications will remain subjective – although it is encouraging that BWH and AM agreed on the visual classifications. And it remains difficult to ascertain which object is in the foreground in a visual classification.

## 5 CATALOGUE

We have classified the blended spectra by the best-fitting templates (PG=passive template, ELG=emission line template) denoting them with Foreground+Background best-fitting template. Out of 280 galaxies, we identify 104 lens candidates, PG with ELG at higher redshifts (PG+ELG); 71 ideal occulting galaxy pairs, ELG in front of a PG (ELG+PG); 78 occulting pairs with both foreground and background galaxies showing strong emission lines, ELG+ELG; and 27 double passive occulting pairs (PG+PG), with both galaxies having passive template fits (Table 1). Fig. 5 shows the distribution of foreground and background galaxy best-fitting templates. We characterize PG+ELG pairs as possible lensing pairs as this is how the SLACS survey found the majority of their strong gravitational lensing pairs, confirmed with *HST* imaging (Koopmans et al. 2006; Treu et al. 2006, 2009; Gavazzi et al. 2007, 2008; Bolton et al. 2008a,b). There is a preference for template 40 in the case of foreground galaxies. We interpret this as a selection effect; it is easier to identify anomalous emission lines on top of a passive spectrum (template 40 has the weakest emission lines). Apart from the preference for template 40 for foreground objects, the distribution is relatively similar. The AUTOZ classification is not particularly biased against either combination of spectra in a blend.

Fig. 6 shows the distribution of redshifts for both the foreground and background galaxies in the blended spectra. Background galaxy redshifts peak around $z = 0.3$ and foreground galaxies a little below that. Similar to the redshift completeness of the GAMA survey

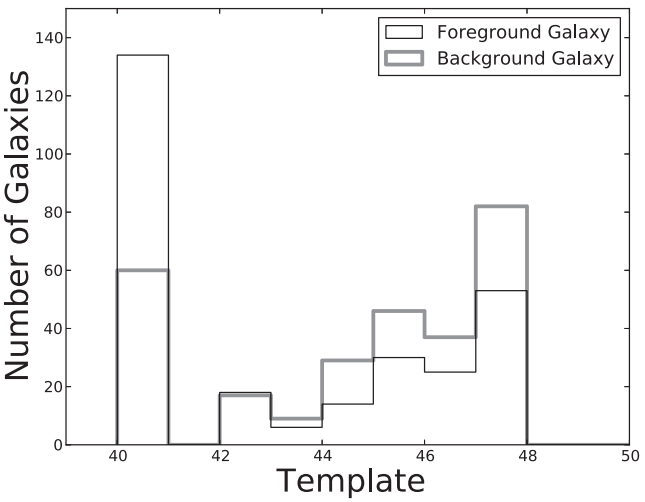


**Figure 5.** The distribution of GAMA spectroscopic best template for the blended spectra catalogue. The templates are numbered from 40–47 in order of increasing emission-line strength. To broadly classify the templates, we select templates 40–42 as 'PG' and 43–47 as 'ELG'.

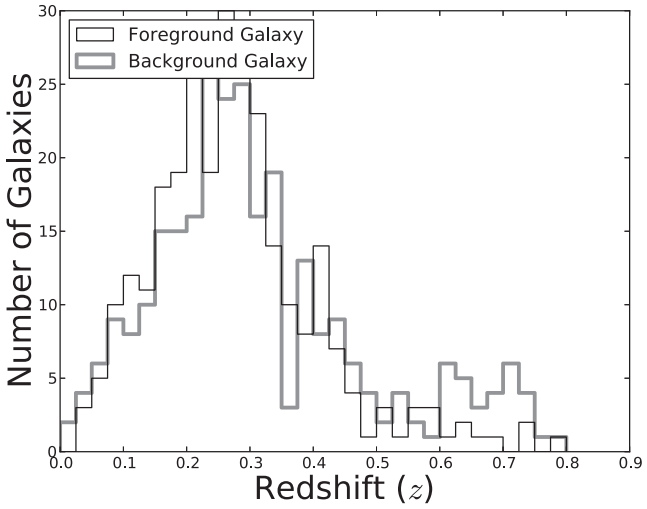


**Figure 6.** The distribution of GAMA spectroscopic redshifts for the blended spectra catalogue. AUTOZ excludes redshift candidates within 600 km s$^{-1}$ of another redshift by design.

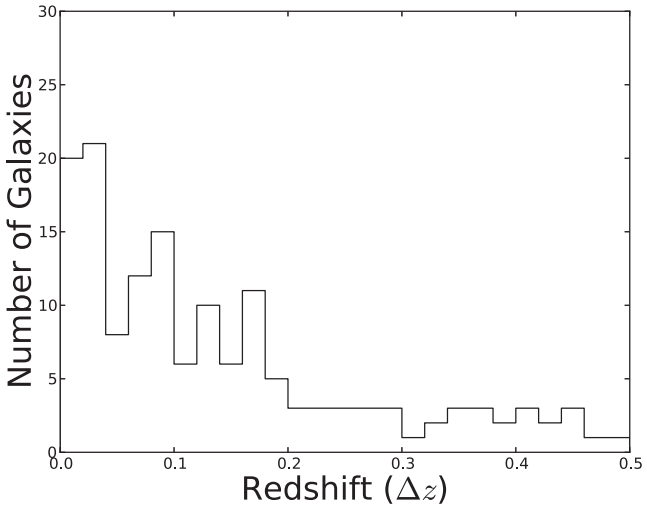


**Figure 7.** The difference in redshift between the foreground and background galaxies in blended spectra catalogue.

(Baldry et al. 2014; Liske 2015), the sample is complete for $z < 0.4$ regardless of template but objects can still be detected out to $z < 0.8$, beyond which the AUTOZ are limited because of a lack of information in the GAMA spectra. The pair members are typically well separated in redshift ($\Delta z > 600$ km s$^{-1}$). Fig. 7 shows the redshift difference for the blended spectra, making these ideal pairs for either lensing studies or as occulting galaxies (see Fig. 8 for the distribution of foreground and background redshifts of either kind).

To classify the pairs into strong lens candidates (PG+ELG) and ELG+PG, ELG+ELG, and PG+PG occulting pairs, we employ the best template fits. Lenses (PG+ELG) are difficult to verify from ground-based imaging, but Arneson, Brownstein & Bolton (2012) argue that spectroscopic selection of lenses are both complete and relatively unbiased within the Einstein ring. Therefore, the list of lenses presented here, especially those in the G23 field (not covered by SDSS), are new candidates for possible *HST* follow-up. Fig. 9 shows some random examples of 'ideal' occulting pairs (ELG+PG) and Fig. 10 of possible strong lenses (PG+ELG). In Holwerda et al. (2007c), we found that 86 out of 101 candidates from SLACS were

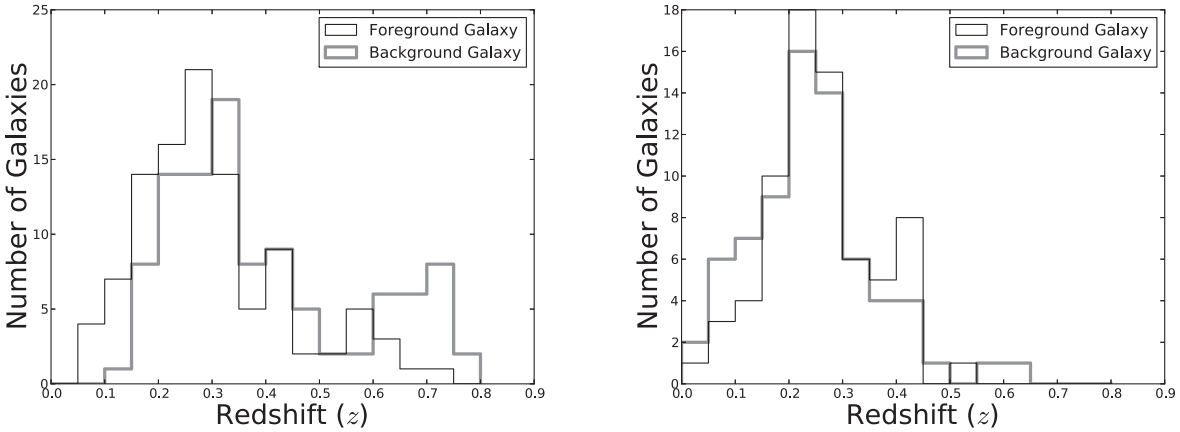


**Figure 8.** The distribution of foreground galaxy redshift and background galaxy redshift for the passive foreground with emission-line background templates (PG+ELG, left-hand panel) and the emission-line foreground template with a passive template for the background objects (ELG+PG, right-hand panel).

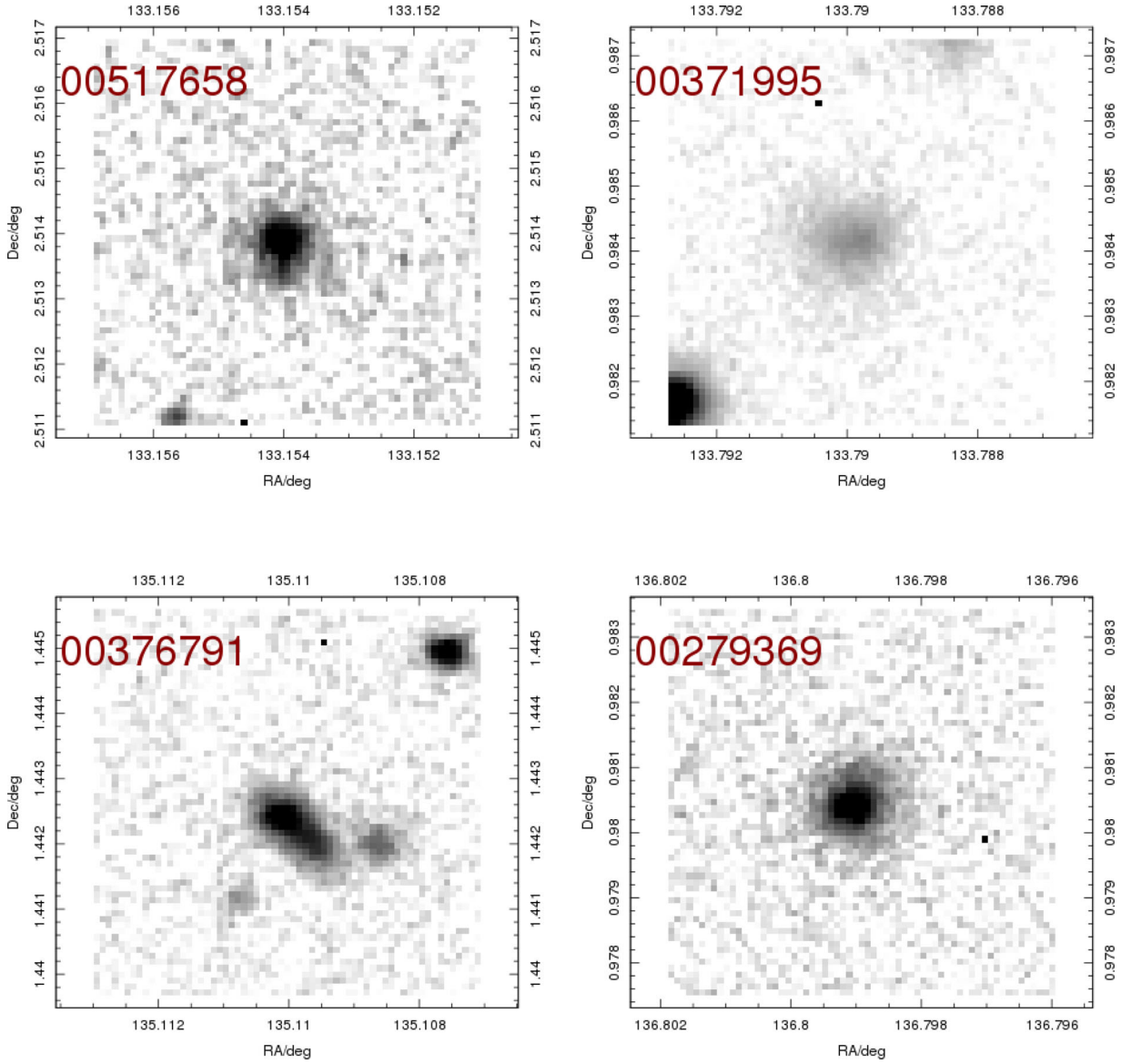


**Figure 9.** Examples of the ELG+PG pairs. SDSS-*i* image cutouts retrieved using http://ict.icrar.org/cutout/. Standard cutout size is 20 arcsec. GAMA id numbers are in red.

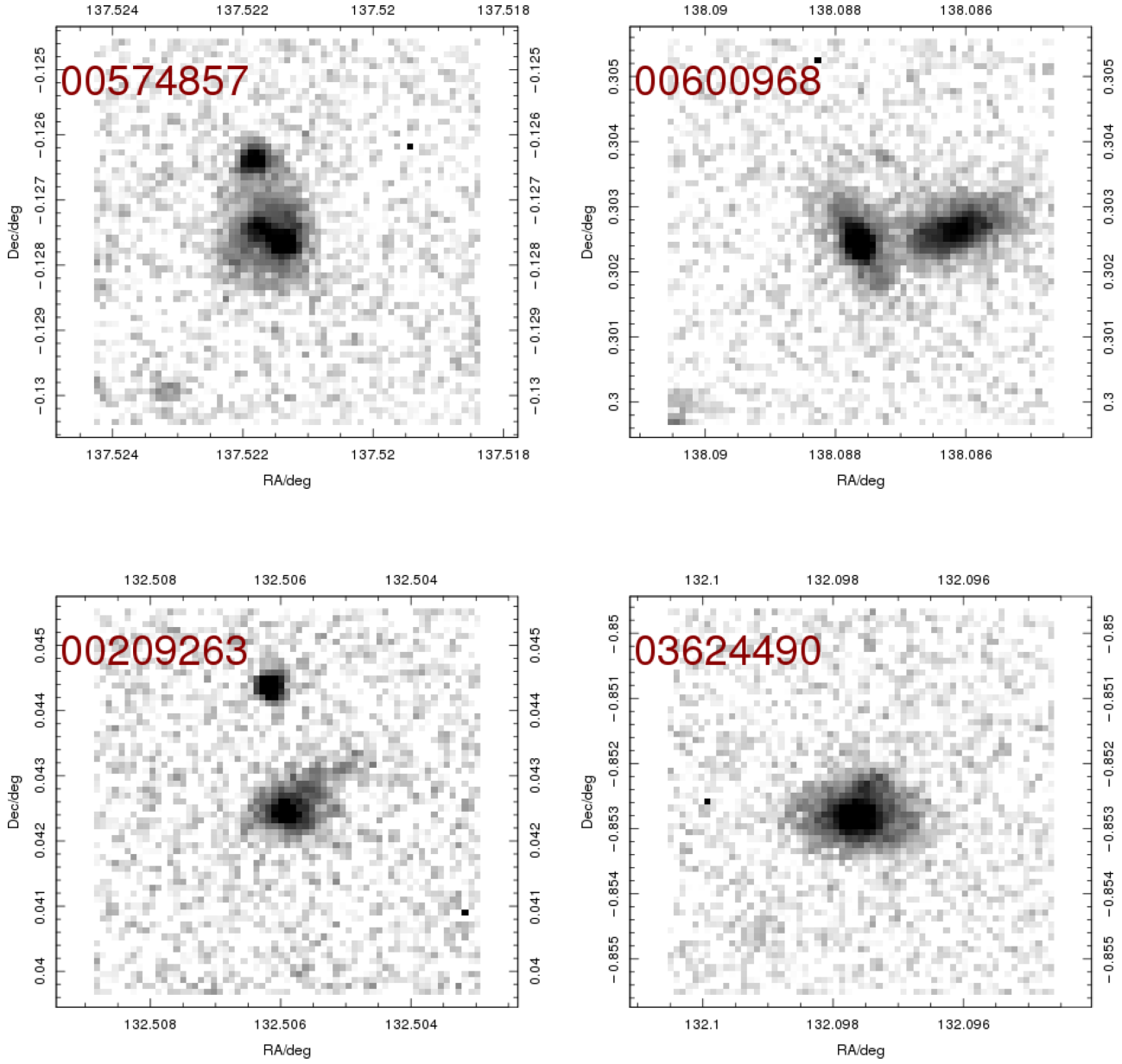


**Figure 9** – *continued*

usable occulting pairs. Fig. 9 shows that indeed most of the spectroscopically identified occulting pairs have a good geometry to extract, in principle, the transmissivity of the foreground galaxies. These new pairs will be of use to model the transmission of the foreground galaxy with a very low impact parameter (almost perfectly aligned galaxies). Alternate occulting galaxy pairs are the ELG+ELG type, which can be used to extract transmission though the foreground galaxy in the bluer wavelengths. For example, Keel et al. (2014) use such spiral-spiral pairs to infer the extinction law in the ultraviolet. This can only be done with a UV-bright spiral as the background galaxy. Intrinsic asymmetry in spiral structure of both pair members introduces uncertainty in the transmission/opacity measurement, but does not introduce a bias. However, irregular galaxies cannot be used as background illuminators. The ELG+ELG occulters are therefore a useful subsample of the occulting pairs. Certainly, one is a clear ELG+ELG pair but many other include an irregular as well. Lastly, we have PG+PG pairs, where both galaxies lack emission lines. These may be lenses still, but are unlikely to attract follow-up attention. As occulting galaxies they are not likely to reveal much new information about the dusty ISM in early types.

## 6 CONCLUDING REMARKS

From the ∼230 000 objects with spectroscopy in the GAMA survey, we identified 280 blended objects (∼0.12 per cent). In contrast, out of the 849 920 spectra in SDSS/DR4 (Adelman-McCarthy et al. 2006), Bolton et al. (2008a) identified a total of 89 lenses and Holwerda et al. (2007c) identified 101 candidates occulting galaxy pairs, i.e. 0.02 per cent of all the SDSS spectra were blends. To make an honest comparison, we can only count the early-type, passive spectra with emission line at different redshift, the target of Bolton et al. (2004) and the subsequent SLACS survey. In GAMA, we identify 104+71=179 of these (0.08 per cent), a factor 4 higher detection rate.

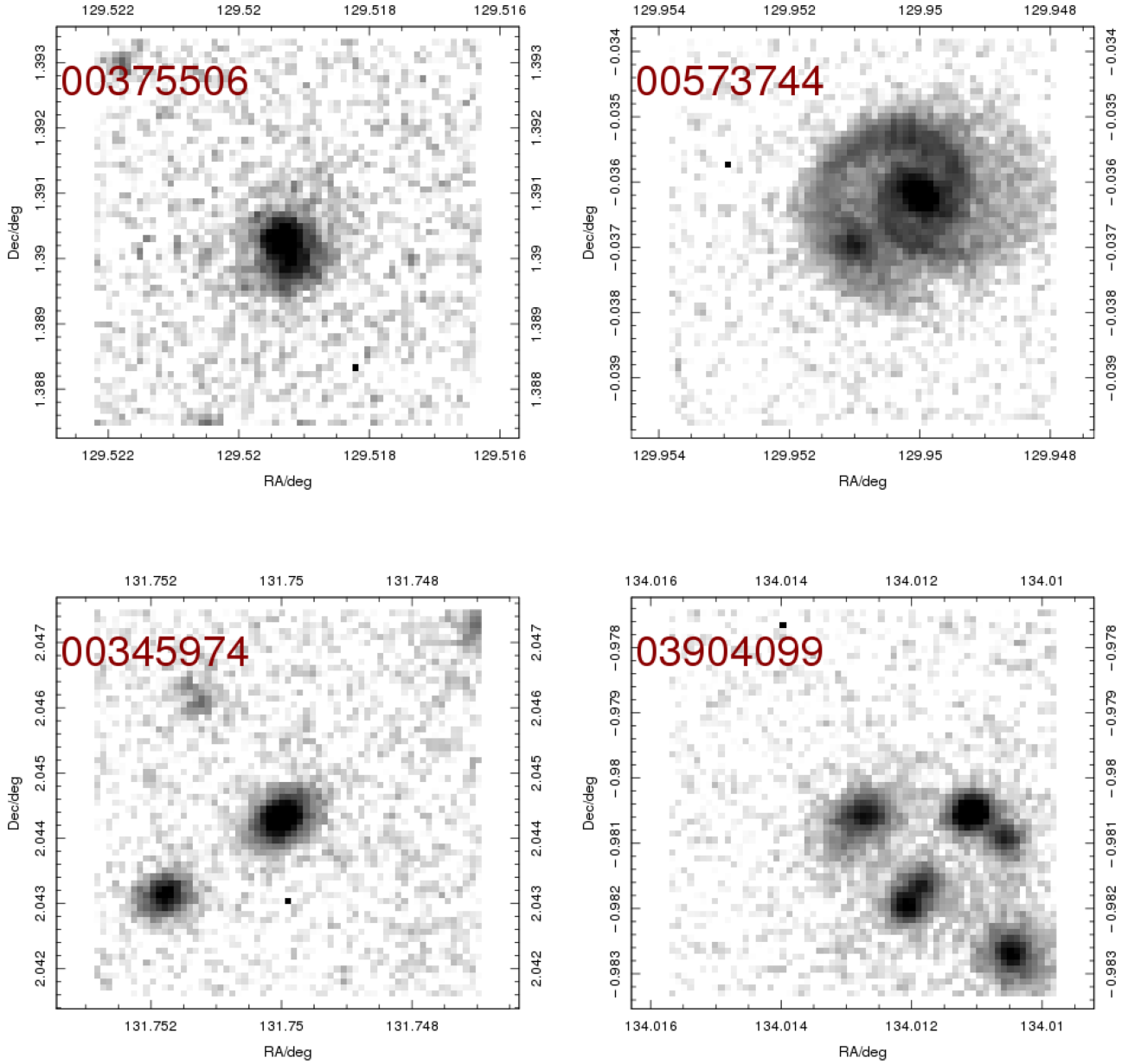


**Figure 10.** Examples of the ELG+ELG pairs. SDSS-*i* image cutouts retrieved using http://ict.icrar.org/cutout/. Standard cutout size is 20 arcsec. GAMA id numbers are in red. ELG include irregulars which limit the use of this class of objects in follow-up analysis.

There are obvious differences between the SDSS and GAMA redshift surveys; a fainter limiting magnitude and a higher completeness (by design) for the GAMA survey. The fainter depth by 2 mag means that there are about 10 times as many galaxies with a similar magnitude (e.g. $r \sim 19.5$ for GAMA, $r \sim 17.5$ for SDSS main galaxy sample). This will result in more blended spectra despite the fact the AAOmega apertures are 2 arcsec compared to 3 arcsec for SDSS. This latter difference diminishes the GAMA survey's sensitivity to overlapping pairs; a wider aperture includes more flux from the outskirts of the occulting galaxy. Naively, one would therefore expect a factor of ∼4.5 improvement in sensitivity of GAMA with respect to SDSS for blended spectra, which bears out approximately (0.12 per cent of GAMA versus 0.02 per cent of SDSS/DR4), better than the increase in blended spectra from SDSS DR4 to DR10. Another difference between the surveys is the identification of the redshift blend. In the SLACS survey, potentially lensed star-forming galaxies are detected through the presence of background oxygen and hydrogen nebular emission lines in the SDSS-DR4 spectra of massive foreground galaxies. The GAMA identification, this paper, is through a complete-spectrum cross-correlation with different templates, which uses the full spectral range to identify redshift, and allows for two blended passive spectra or at least does not require very strong emission lines at different redshifts.

There are several possible uses for these blended spectral galaxy pairs.

The occulting pairs in GAMA are added to the master occulting galaxy catalogue, predominantly based on the SDSS spectral identifications (86 blended pairs in Holwerda et al. 2007c), and the GalaxyZoo identifications (1993, Keel et al. 2013).

The presented catalogue of occulting pairs constitutes one way to identify occulting pairs in GAMA. Another approach uses the

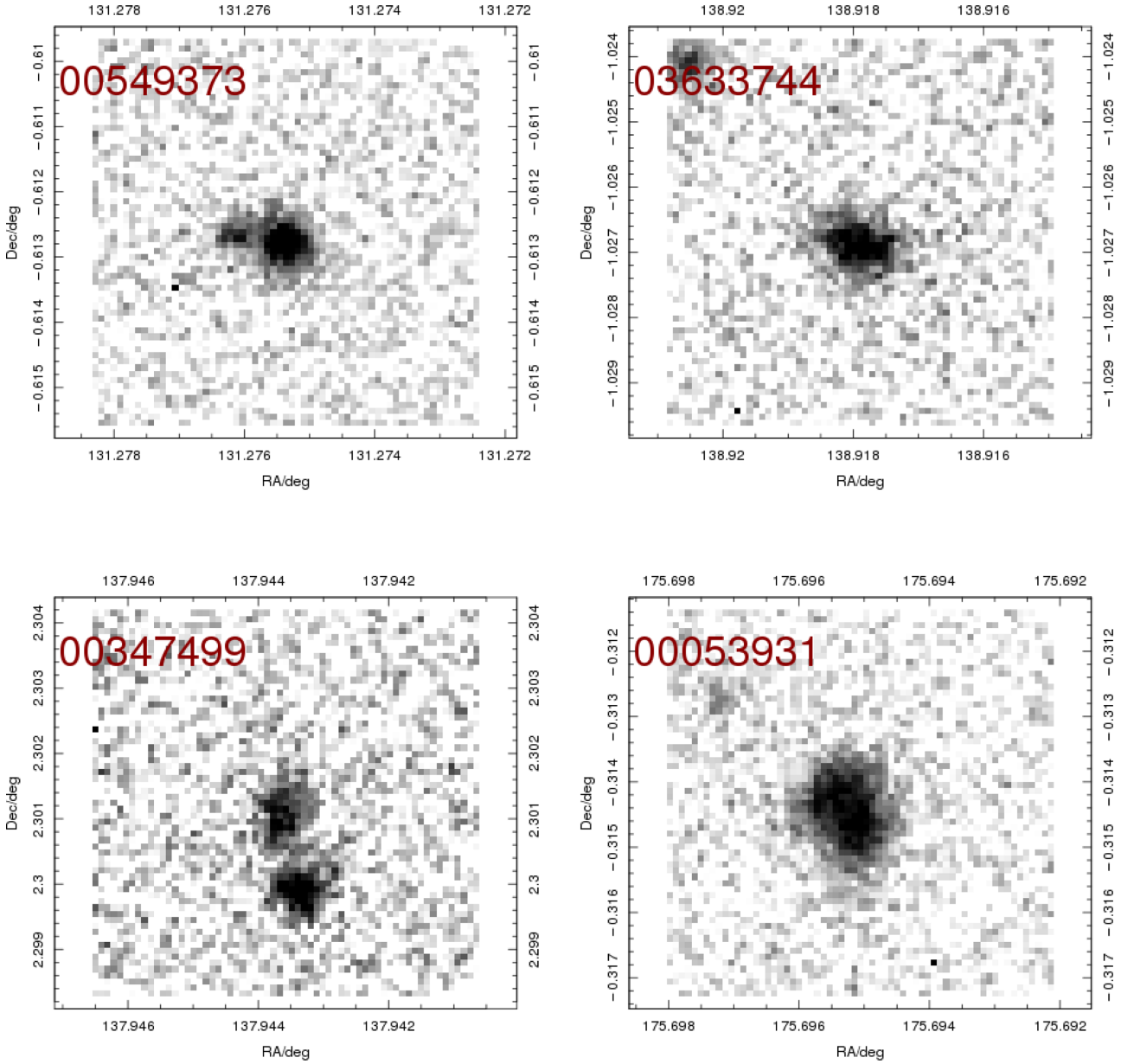


**Figure 10** – *continued*

rejects from the pairs and group catalogue; galaxy pairs that are close on the sky but separated enough to warrant separate fibre assignment and do not exhibit a blended spectrum. By requiring that both pair members are well-separated in redshift, we obtain bona fide occulting pairs.

A complete catalogue of galaxy groups is one of the primary goals of the GAMA survey (Robotham et al. 2011, 2014). A second sample of overlapping pairs will be identified from this catalogue, once it is complete (∼300 expected). Therefore, between the high-fidelity automated identification of shared-fibre pairs and simultaneously, a complete census of close, serendipitous overlaps with separate redshifts, the GAMA identifications of overlapping galaxies will be the most complete to date.

In the case of the lenses, the presented lensing galaxy candidates represent a near doubling of the known objects from SLACS (89 lenses) and a useful addition to the BOSS identified ones (Bolton et al. 2012). The increased depth and completeness of GAMA means more distant and lower mass lenses are included. It should be illustrative to study these blended objects with the ongoing IFU surveys (e.g. Sydney-Australian-Astronomical-Observatory Multi-object Integral-Field Spectrograph/Mapping Nearby Galaxies at APO) and perhaps spatially separate the blended spectral signal or at least study the variation with fibre of the blended signal. For a full lensing analysis, the imaging will have to be higher spatial resolution than those available from either SDSS, KiDS or any of the other imaging surveys available for GAMA. Either dedicated Very Large Telescope/Adaptive Optics observations or *HST* imaging would fit the bill. The benefits of the GAMA selection are lower mass lenses and lensed images closer to the lensing galaxy.

## ACKNOWLEDGEMENTS

The authors thank the referee for his or her comments and suggestions. The lead author thanks the European Space Agency for

the support of the Research Fellowship programme and the whole GAMA team for a magnificent observational effort. GAMA is a joint European-Australasian project based around a spectroscopic campaign using the Anglo-Australian Telescope. The GAMA input catalogue is based on data taken from the SDSS and the United Kingdom Infrared Telescope Infrared Deep Sky Survey. Complementary imaging of the GAMA regions is being obtained by a number of independent survey programmes including *GALEX* MIS, VST KiDS, VISTA VIKING,WISE, *Herschel*-ATLAS, GMRT and ASKAP providing UV to radio coverage. GAMA is funded by the STFC (UK), the ARC (Australia), the AAO, and the participating institutions. The GAMA website is www.gamasurvey.org/. MJIB acknowledges financial support from the Australian Research Council (FT100100280) This research has made use of the NASA/IPAC Extragalactic Database (NED) which is operated by the Jet Propulsion Laboratory, California Institute of Technology, under contract with the National Aeronautics and Space Administration. This research has made use of NASA's Astrophysics Data System.

## REFERENCES

Adelman-McCarthy J. K. et al., 2006, ApJS, 162, 38
Albrecht A. et al., 2006, preprint (astro-ph/0609591)
Andredakis Y. C., van der Kruit P. C., 1992, A&A, 265, 396
Arneson R. A., Brownstein J. R., Bolton A. S., 2012, ApJ, 753, 4
Baes M. et al., 2010, A&A, 518, L39
Baldry I. K. et al., 2010, MNRAS, 404, 86
Baldry I. K. et al., 2014, MNRAS, 441, 2440
Bendo G. J. et al., 2012, MNRAS, 419, 1833
Bendo G. J. et al., 2015, MNRAS, 448, 135
Berlind A. A., Quillen A. C., Pogge R. W., Sellgren K., 1997, AJ, 114, 107
Bianchi S., Xilouris E. M., 2011, A&A, 531, L11
Bolton A. S., Burles S., Schlegel D. J., Eisenstein D. J., Brinkmann J., 2004, AJ, 127, 1860
Bolton A. S., Burles S., Koopmans L. V. E., Treu T., Moustakas L. A., 2006, ApJ, 638, 703
Bolton A. S., Burles S., Koopmans L. V. E., Treu T., Gavazzi R., Moustakas L. A., Wayth R., Schlegel D. J., 2008a, ApJ, 682, 964
Bolton A. S., Treu T., Koopmans L. V. E., Gavazzi R., Moustakas L. A., Burles S., Schlegel D. J., Wayth R., 2008b, ApJ, 684, 248
Bolton A. S. et al., 2012, ApJ, 757, 82
Brownstein J. R. et al., 2012, ApJ, 744, 41
Cuillandre J., Lequeux J., Allen R. J., Mellier Y., Bertin E., 2001, ApJ, 554, 190
de Jong J. T. A., Verdoes Kleijn G. A., Kuijken K. H., Valentijn E. A., 2013, Exp. Astron., 35, 25
de Looze I. et al., 2012, MNRAS, 427, 2797
Domingue D. L., Keel W. C., Ryder S. D., White R. E., III, 1999, AJ, 118, 1542
Domingue D. L., Keel W. C., White R. E., III, 2000, ApJ, 545, 171
Draine B. T. et al., 2014, ApJ, 780, 172
Driver S. P. et al., 2009, Astron. Geophys., 50, 050000
Driver S. P. et al., 2011, MNRAS, 413, 971
Elmegreen D. M., Kaufman M., Elmegreen B. G., Brinks E., Struck C., Klarić M., Thomasson M., 2001, AJ, 121, 182
Galametz M. et al., 2012, MNRAS, 425, 763
Gavazzi R., Treu T., Rhodes J. D., Koopmans L. V. E., Bolton A. S., Burles S., Massey R. J., Moustakas L. A., 2007, ApJ, 667, 176
Gavazzi R., Treu T., Koopmans L. V. E., Bolton A. S., Moustakas L. A., Burles S., Marshall P. J., 2008, ApJ, 677, 1046
González R. A., Allen R. J., Dirsch B., Ferguson H. C., Calzetti D., Panagia N., 1998, ApJ, 506, 152
González R. A., Loinard L., Allen R. J., Muller S., 2003, AJ, 125, 1182
Hinz J. L., Engelbracht C. W., Willmer C. N. A., Rieke G. H., Rieke M. J., Smith P. S., Blaylock M., Gordon K. D., 2009, in K. Sheth, A. Noriega -Crespo, J. Ingalls, and R. Paladini, eds, The Evolving ISM in the Milky Way and Nearby Galaxies. Available at: http://ssc.spitzer.caltech.edu/mtgs/ismevol/
Hinz J. L. et al., 2012, ApJ, 756, 75
Holwerda B. W., 2005, PhD thesis, Rijksuniversiteit Groningen
Holwerda B. W., 2008, MNRAS, 386, 475
Holwerda B. W., Keel W. C., 2013, A&A, 556, A42
Holwerda B. W., González R. A., Allen R. J., van der Kruit P. C., 2005a, AJ, 129, 1381
Holwerda B. W., González R. A., Allen R. J., van der Kruit P. C., 2005b, AJ, 129, 1396
Holwerda B. W., González R. A., Allen R. J., van der Kruit P. C., 2005c, A&A, 444, 101
Holwerda B. W., González R. A., van der Kruit P. C., Allen R. J., 2005d, A&A, 444, 109
Holwerda B. W., González R. A., Allen R. J., van der Kruit P. C., 2005e, A&A, 444, 319
Holwerda B. W. et al., 2007a, AJ, 134, 1655
Holwerda B. W. et al., 2007b, AJ, 134, 2226
Holwerda B. W., Keel W. C., Bolton A., 2007c, AJ, 134, 2385
Holwerda B. W., Keel W. C., Williams B., Dalcanton J. J., de Jong R. S., 2009, AJ, 137, 3000
Holwerda B. W., Allen R. J., de Blok W. J. G., Bouchard A., Gonzalez-Lopezlira R. A., van der Kruit P. C., Leroy A., 2013, Astron. Nachr., 334, 268
Holwerda B. W. et al., 2012, A&A, 541, L5
Holwerda B. W., Böker T., Dalcanton J. J., Keel W. C., de Jong R. S., 2013, MNRAS, 433, 47
Holwerda B. W., Reynolds A., Smith M., Kraan-Korteweg R. C., 2015, MNRAS, 446, 3768
Hughes T. M. et al., 2014, A&A, 565, A4
Hughes T. M. et al., 2015, A&A, 575, A17
Keel W. C., White R. E., III, 2001a, AJ, 121, 1442
Keel W. C., White R. E., III, 2001b, AJ, 122, 1369
Keel W. C., Manning A. M., Holwerda B. W., Mezzoprete M., Lintott C. J., Schawinski K., Gay P., Masters K. L., 2013, PASP, 125, 2
Keel W. C., Manning A. M., Holwerda B. W., Lintott C. J., Schawinski K., 2014, AJ, 147, 44
Koopmans L. V. E., Treu T., Bolton A. S., Burles S., Moustakas L. A., 2006, ApJ, 649, 599
Lintott C. J. et al., 2008, MNRAS, 389, 1179
Liske J. et al., 2015, MNRAS, submitted
Popescu C. C., Misiriotis A., Kylafis N. D., Tuffs R. J., Fischera J., 2000, A&A, 362, 138
Popescu C. C., Tuffs R. J., Dopita M. A., Fischera J., Kylafis N. D., Madore B. F., 2011, A&A, 527, A109
Robotham A. S. G. et al., 2011, MNRAS, 416, 2640
Robotham A. S. G. et al., 2014, MNRAS, 444, 3986
Saunders A., Goldman D. I., Full R. J., Buehler M., 2006, in Gerhart G. R., Shoemaker C. M., Gage D. W., eds, Proc. SPIE Conf. Ser. Vol. 6230, Unmanned Systems Technology VIII. SPIE, Bellingham, p. 17
Sharp R. et al., 2006, in McLean I. S., Iye M., eds, Proc. SPIE Conf. Ser. Vol. 6269, Ground-based and Airborne Instrumentation for Astronomy. SPIE, Bellingham, p. 62690
Smith M. W. L. et al., 2010, A&A, 518, L51
Treu T., Koopmans L. V., Bolton A. S., Burles S., Moustakas L. A., 2006, ApJ, 640, 662
Treu T., Gavazzi R., Gorecki A., Marshall P. J., Koopmans L. V. E., Bolton A. S., Moustakas L. A., Burles S., 2009, ApJ, 690, 670
Verstappen J. et al., 2013, A&A, 556, A54
White R. E., Keel W. C., 1992, Nature, 359, 129
White R. E., III, Keel W. C., Conselice C. J., 2000, ApJ, 542, 761
Xilouris E. M. et al., 2012, A&A, 543, A74

## SUPPORTING INFORMATION

Additional Supporting Information may be found in the online version of this article:

**Table 3**. The complete catalogue of blended spectra in the GAMA survey (http://mnras.oxfordjournals.org/lookup/suppl/doi:10.1093/mnras/stv589/-/DC1).

Please note: Oxford University Press are not responsible for the content or functionality of any supporting materials supplied by the authors. Any queries (other than missing material) should be directed to the corresponding author for the article.

This paper has been typeset from a TEX/LATEX file prepared by the author.